Mausam, (1992), **43**, 3, 283-290

551.551 : 551.510.522

Wind and turbulence profiles in a simulated wind tunnel boundary layer

S. SIVARAMAKRISHNAN and BRIJ MOHAN
Indian Institute of Tropical Meteorology, Pune
(Received 27 May 1991)

सार — निम्न गति लघु परीक्षण अनुभाग (0.61 मी × 0.61 मी) पवन सुरंग के खुरदरे तल पर, कृत्रिम रूप से, मोटे (32 सें० मी०) प्रक्षोभ परिसीमा स्तर की वृद्धि को बढ़ाने के लिए हनीकोम चपटे प्लेट ग्रिड और बेलनाकार छड़ों की प्रणाली का विकास किया गया। पवन वेग, अनुदैर्ध्य प्रक्षोभ सघनता और रेनल्ड्स प्रतिबल के अनुकारित कार्यों को प्रतिरूपी ग्रामीण भूभाग पर निष्प्रभावी वायु मंडलीय परिसीमा स्तर के समरूप दिखाने के लिए प्रस्तुत किया गया है। सुरंग तल पर 10, 30 और 100 मि० मी० पर मापित प्रक्षोभ के अनुदैर्ध्य स्पैक्ट्रम को वायुमंडलीय स्पैक्ट्रम के साथ सही तुलना करने के लिए प्रस्तुत किया गया और स्पैक्ट्रम के जड़त्व उपपरिसर में कोलमोगो राफ्स के — 2/3 नियम के साथ निकट रूप से अनुकूल पाए गए है। स्पैक्ट्रम द्वारा आकलित अनुदैर्ध्य प्रक्षोभ के दैर्ध्य मापक्रम पर आधारित पर्यावरणीय कठिनाईयों के प्रयोगशाला संबंधी निदर्शन के लिए 1 : 900 के मापक्रम का प्रस्ताव रखा गया जिसमें निष्प्रभावी वायुमंडलीय सतह स्तर में द्रव्यमान का वहन, मात्र यांत्रिकी मूल के भंवरों के कारण होता है।

ABSTRACT. A system of Honeycomb Flat Plate (HFP) grid and cylindrical rods has been developed to accelerate the growth of a thick (32 cm) turbulent boundary layer, artificially, over rough floor of a low speed short test-section (0.61 m × 0.61 m) wind tunnel. Simulated profiles of wind velocity, longitudinal turbulence intensity and Reynolds stress are shown to have similarity to those of a neutral atmospheric boundary layer over a typical rural terrain. Longitudinal spectrum of turbulence measured at 10, 30 and 100 mm above tunnel floor is shown to compare well with atmospheric spectrum and agree closely with the Kolmogoroff's —2/3 law in the inertial sub-range of the spectrum. Based on the length scale of longitudinal turbulence estimated from the spectrum, a scale of 1:900 has been proposed for laboratory modelling of environmental problems wherein the transport of mass in a neutral atmospheric surface layer is solely due to eddies of mechanical origin.

Key Words — Atmospheric boundary layer, Wind tunnel, Honeycomb flat plate, Hot wire anemometer, Spectrum analyser, Turbulence

1. Introduction

Laboratory simulation of adiabatic atmospheric boundary layer in wind tunnels is a pre-requisite to model the environmental problems like dispersion of air pollutants, flow characteristics in wind energy and wind loading studies. It employs the technique of developing a thick boundary layer naturally over a long fetch of roughness in a long wind tunnel (Cermak 1970), or artificially in short test-section wind tunnels by means of grids, rods, plates, vortex generators (Lloyd 1967, Counihan 1969, Cook 1978, Okamoto 1986, 1987). Majority of contemporary simulation methods employ the technique compromising between the two in which a natural boundary layer is allowed to develop over an intermediate length of rough wall after giving an initial start by means of barriers and mixing devices.

In the present study, a thick boundary layer is developed in a short test section wind tunnel using two cylindrical rods and a Honeycomb Flat Plate (HFP) grid as a barrier cum mixing device. Characteristics of profiles of mean velocity, longitudinal turbulence intensity, Reynolds stress and spectrum of longitudinal turbulence generated over a rough floor downstream of HFP are evaluated with respect to their similarity to those over an adiabatic atmospheric boundary layer.

2. Basic approach to HFP grid and experimental details

The geometry of the barrier and mixing device and its position in the stream of air flow decide the distribution of velocity and turbulence downstream of it. Lloyd (1967) used an array of flat plates to produce sheared turbulent flow; but the resultant scale of turbulence produced was small. The scale and decay of turbulence downstream of grids or honeycombs are related to the mesh size (Taylor 1960). Therefore, adoption of a graded honeycomb to produce sheared turbulent flow is a practical proposition (Lawson 1968). The choice of combining graded honeycomb with an array of flat plates in this experiment is based on the reasoning that, as in the natural atmospheric boundary layer, the turbulence intensity close to the floor shall be larger and also decreasing smoothly with height in the wind tunnel simulated boundary layer. Honeycomb is, therefore, graded with cells of two different dimensions : Cells of 6.35 mm size (to produce small eddies) are fixed at a

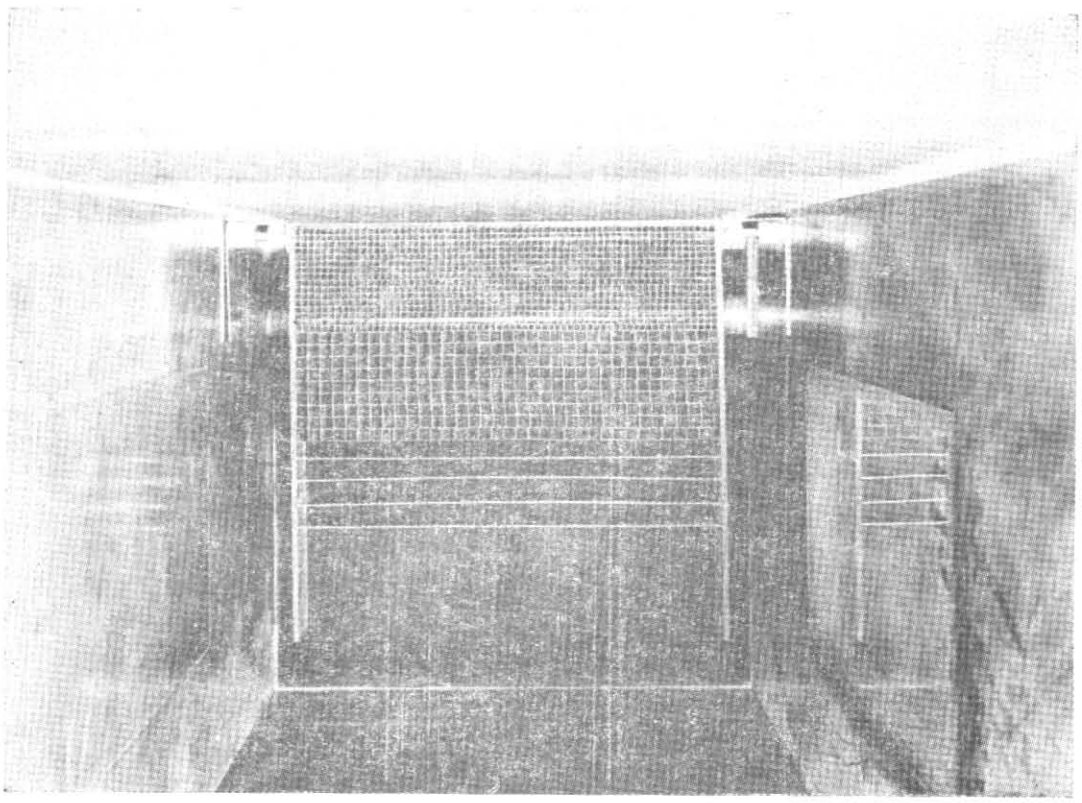

Fig. 1. A view of Honeycomb Flat Plate Grid (HFP) with cylindrical rods infront, inside the test-section of wind tunnel

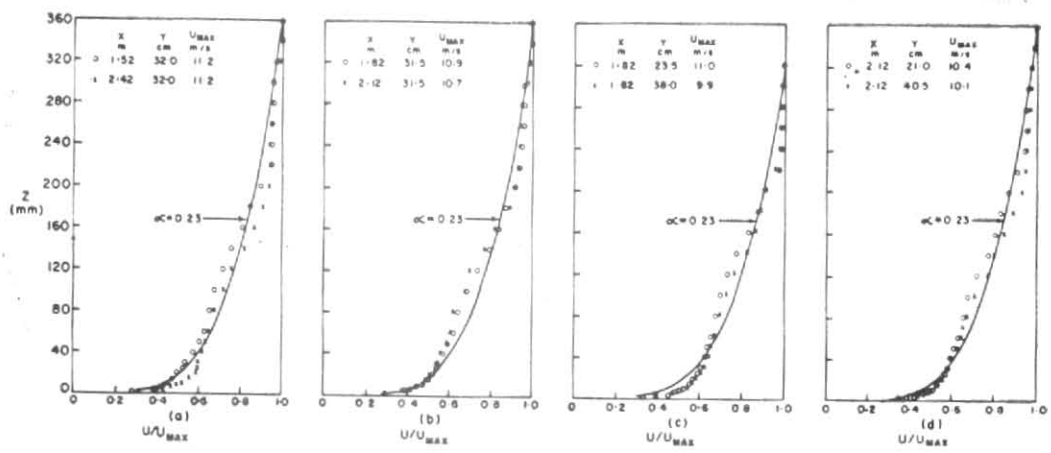

Fig. 2(a). Mean velocity profiles simulated and fitted to the power law wind profile of the atmospheric boundary layer

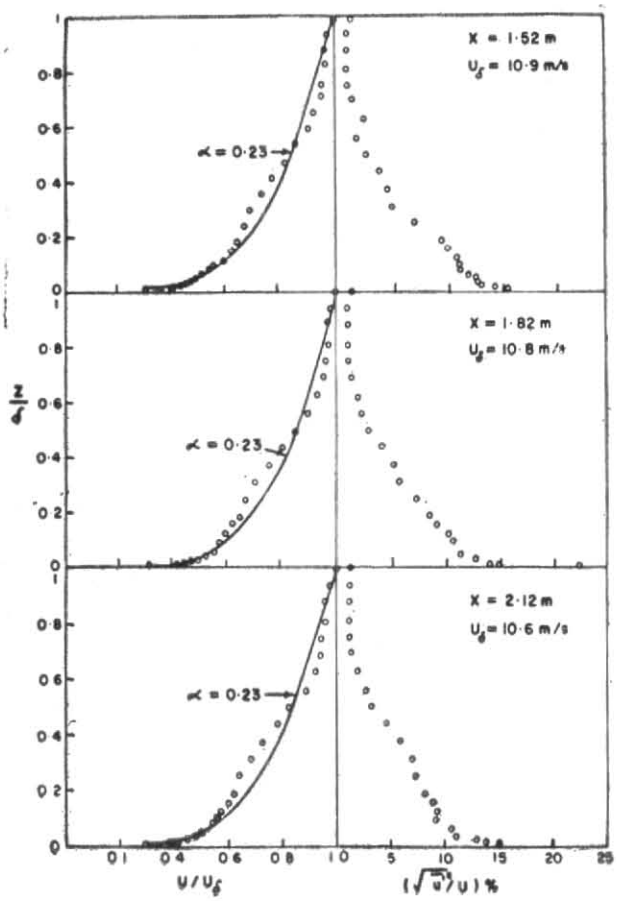

Fig. 2(b). Mean velocity and longitudinal turbulence intensity profiles at different locations downstream along midspan

height of 115 mm inside a 457 mm × 457 mm perspex frame, cells of 12.7 mm size (to produce big eddies) are fixed at a height 120 mm above the array of smaller cells. The cells are 76.2 mm long (depth of honeycomb) and are made of 0.3 mm aluminium sheets. Four aluminium flat plates, 1.65 mm thick, are fixed to the frame at arbitrarily located positions of 20, 45, 70 and 95 mm above the honeycomb array. Such an array of Honeycomb cum Flat Plate is capable of producing sheared turbulent flow with a good distribution of eddy sizes. In an earlier study (Sivaramakrishnan 1980) HFP was installed at the test section entrance and the mean velocity profiles measured at 2.6 m downstream of HFP, over a smooth tunnel floor were found to have similarity to power law wind profile of the adiabatic atmospheric boundary layer. The artificially developed boundary layer was 32-34 cm thick at free stream velocities of 10-12 m/s. However, the streamwise turbulence intensity was found to decrease faster above the floor and that except at the region close to the floor, it was not of the required order when compared with the atmospheric profile. To increase and sustain the turbulence intensity near the floor, the floor was roughened using coarse grade emery paper (C201AH, Carborandum Univeral) in this experiment. Two cylindrical rods of 2.54 cm diameter were installed infront of HFP so that the flow approaching HFP has turbulent wakes generated by the rods. The rods were mounted horizontally at the entrance of test section such that one rests on the floor and the other above at an axis to axis separation of 10 cm. Such an arrangement of the cylindrical barriers is to impart an initial momentum deficit. The HFP grid was mounted downstream at 27.5 cm from the entrance of test section. The turbulent wakes in the flow on passing through HFP get directed by the cells of different mesh size which results in a good distribution of velocity and turbulence intensity in the shear flow downstream, and the rough floor sustains turbulence near the floor. Vertical separation of cylindrical rods in front of HFP was determined by repeating the experiments for different axis-to-axis separation and measuring the turbulence intensity distribution downstream of HFP, where the mean velocity profiles were well developed.

The wind tunnel used for the study was a low speed open circuit tunnel of test section 0.61 m × 0.61 m × 3m, located at the Central Water and Power Research Station (CWPRS), Khadakwasla, Pune. Emery coarse paper of thickness 1.2 mm, pasted on to a long 6.35 mm thick plywood plate, was fitted on the test section floor along its entire length. Rear view of cylindrical rods and HFP along with rough tunnel floor is shown in Fig. 1. The tunnel was run at a free stream speed of 10-11 m/s and the velocity profiles measured at several locations downstream of HFP. Thermo Systems Incorporated, U.S.A. (TSI), Model 1054A constant temperature anemometer, Model 1076 true r.m.s. voltmeter and Model 1015C correlator were used with single or x-type hotwire boundary layer probes to measure the mean velocity, turbulence intensity and Reynolds stress profiles. TSI hot wire sensor is a platinum plated tungsten wire of 4 micron diameter, 1.3 mm length and has frequency response from DC-200 KHz in air at 100 m/s. A three-dimensional precision traverse was used to traverse the probes. To measure the streamwise power spectral density function of turbulence, a Bruel and Kjaer Type 2010 heterodyne analyzer of frequency range 2 Hz to 200 KHz was used. Spectral density was measured at heights of 10, 30 and 100 mm above the tunnel floor. Choosing x-axis along the stream of flow the location of points along x is measured *w.r.t.* the rear face of HFP. The y-axis refers to the cross stream (lateral), *i.e.*, span distance measured from the interior wall of test section on the observer's side of the tunnel. The z-axis refers to the vertical, *i.e.*, the height *w.r.t.* the rough floor of the tunnel.

3. Results

Mean velocity and turbulence profiles at several downstream locations were measured from 2 mm above the tunnel floor using a boundary layer type single hot wire probe.

3.1. *Profiles of mean velocity and longitudinal turbulence intensity*

Mean velocity profiles measured downstream of HFP are shown in Fig. 2(a). The profiles start developing at 1.52 m and attain equilibrium at 1.82-2.12 m. Spanwise distribution of profiles at 1.82 and 2.12 m is nearly uniform. Fig. 2(b) depicts the profiles (height z normalized with δ — the boundary layer height) of mean velocity (U) and longitudinal turbulence intensity

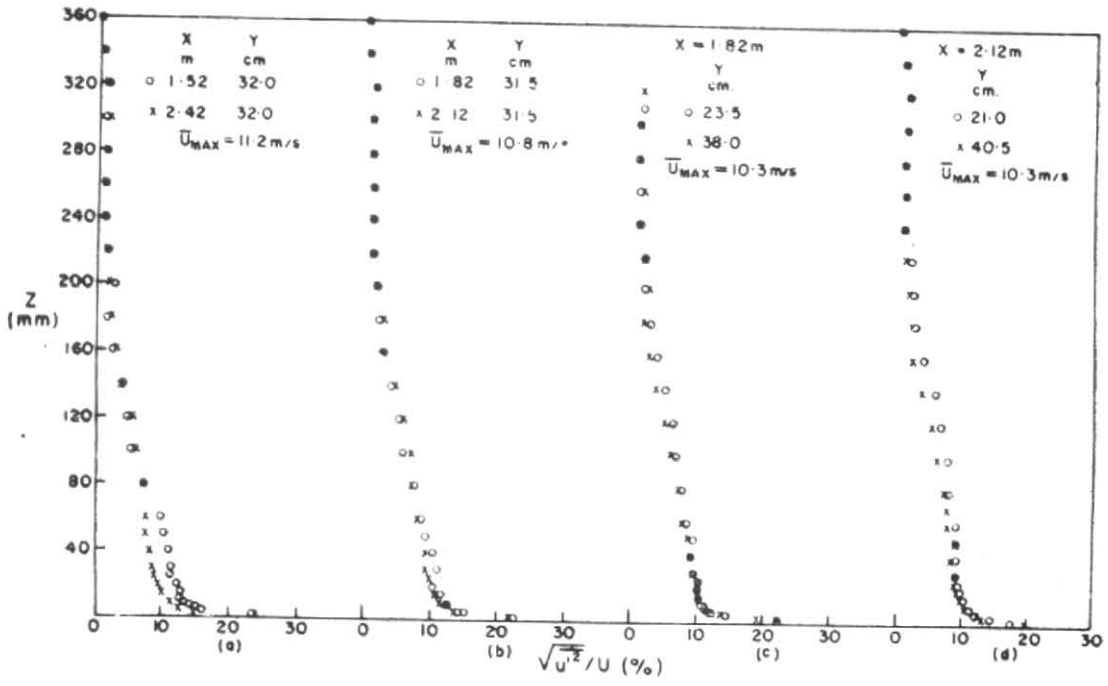

Fig. 3. Simulated profiles of longitudinal turbulence intensity

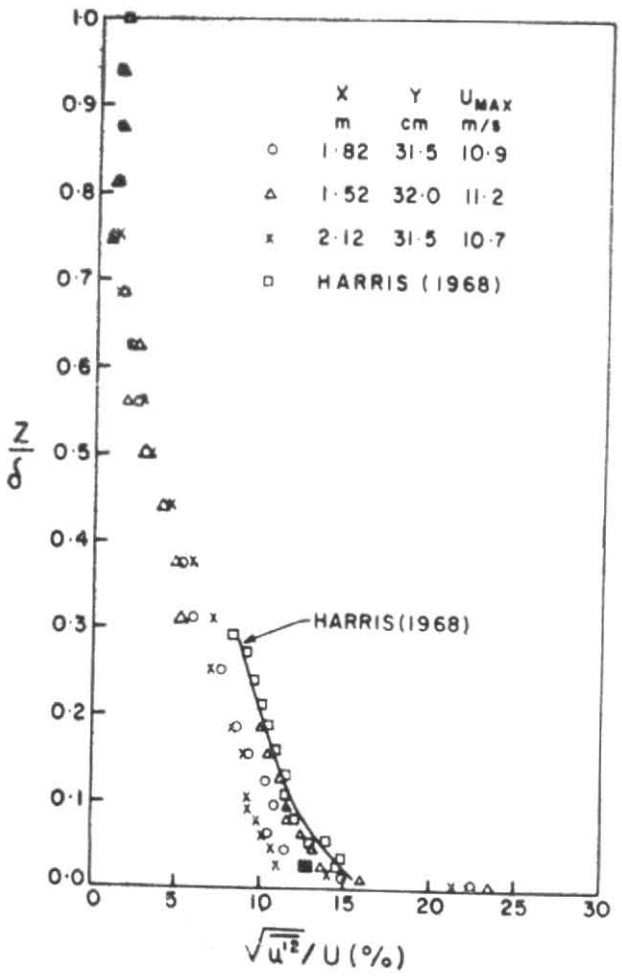

Fig. 4. Profiles of longitudinal turbulence intensity compared with Harris' atmospheric profile

along midspan at three different points downstream of HFP. The mean velocity and turbulence intensity profiles at 1.82 m downstream show relatively better shape than those at 1.52 and 2.12 m. The boundary layer developed is quite thick (δ=32 cm) at these locations. A power law profile :

$$(U/U_\delta) = (Z/\delta)^{\alpha} \qquad (1)$$

with power exponent $\alpha = 0.23$ typical over rough terrain (Counihan 1975) has been fitted to these velocity profiles. The points in the lower 1/5th of the measured profiles fit $\alpha = 0.23$ profile very closely U_δ is the wind velocity at the height of boundary layer usually defined as the height where the velocity is 98% of free stream velocity. The shape of all these profiles reveals that the boundary layer is turbulent.

Profiles of longitudinal turbulence intensity show that close to the floor (Z=2mm) it is as high as 23% and falls down to 7.5% at Z/δ=0.25. The intensity decreases relatively smoothly at x=1.82 m. Streamwise and spanwise longitudinal turbulence intensity profiles are shown in Fig. 3. It is observed that the profiles are nearly uniform for x=1.82-2.12 m. In Fig. 4, turbulence intensity profile based on fullscale measurements (Harris 1968) for flow of atmospheric boundary layer over rural terrain is drawn alongwith simulated profiles. The agreement is reasonable within 5%.

Fig. 5 shows the logarithmic variation of the velocity profiles in the lower region of the boundary layer (Z/δ=0.25) at x=1.52, 1.82 and 2.12 m. Intercept of the profile with height axis yields an approximate value of the roughness length Z_0 obeying the log-law velocity distribution :

$$U = (u_*/k) \ln (Z/Z_0) \qquad (2)$$

where u_* is the friction velocity and k the Von Karman constant. The intercept yields $Z_0 = 10^{-4}\,\delta$ at x=1.52, 1.82 and 2.12 m in Fig. 4.

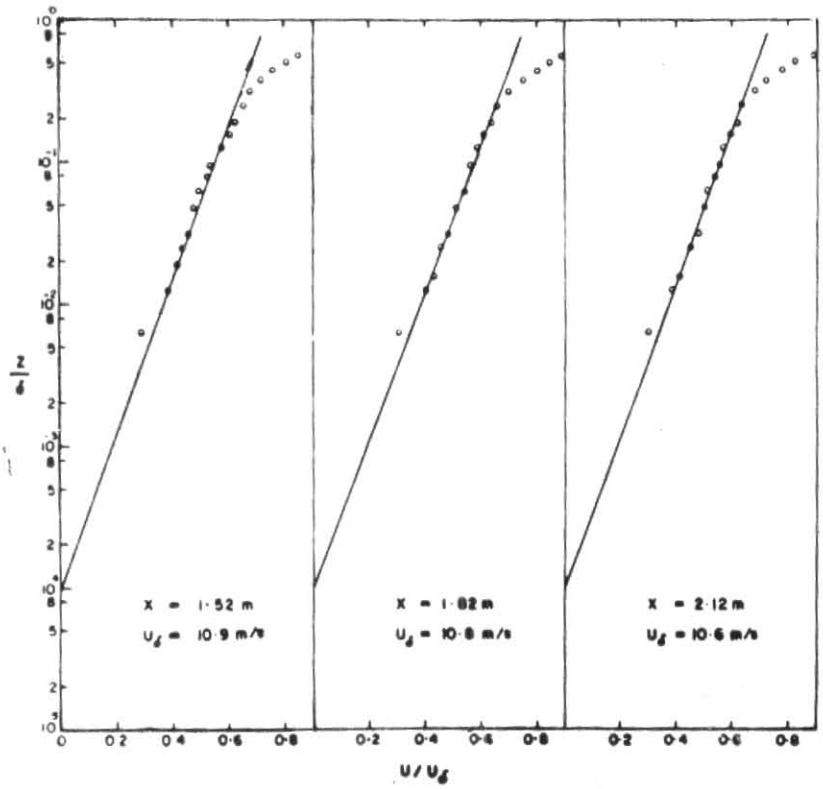

Fig. 5. Mean velocity profiles fitted to logarithmic law of the surface layer

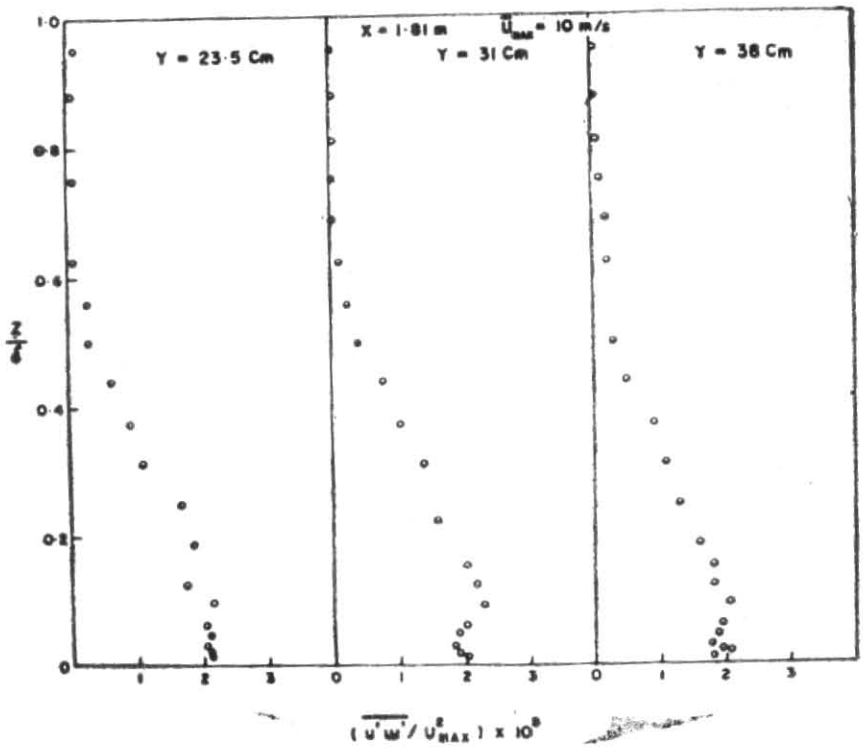

Fig. 6. Simulated profile of Reynolds' stress

3.2. *Profile of Reynolds stress*

The profile of Reynolds stress was measured using a TSI boundary layer type x-wire probe by orienting the hot wire sensors parallel to the xz plane. Fig. 6 shows the plot of Reynolds stress $(\overline{u', \omega'})$ normalized with the square of free stream velocity against height Z normalized with δ, at x=1.82 m. The profile at midspan and at two different points along span are shown reasonably close to the floor the mean Reynolds

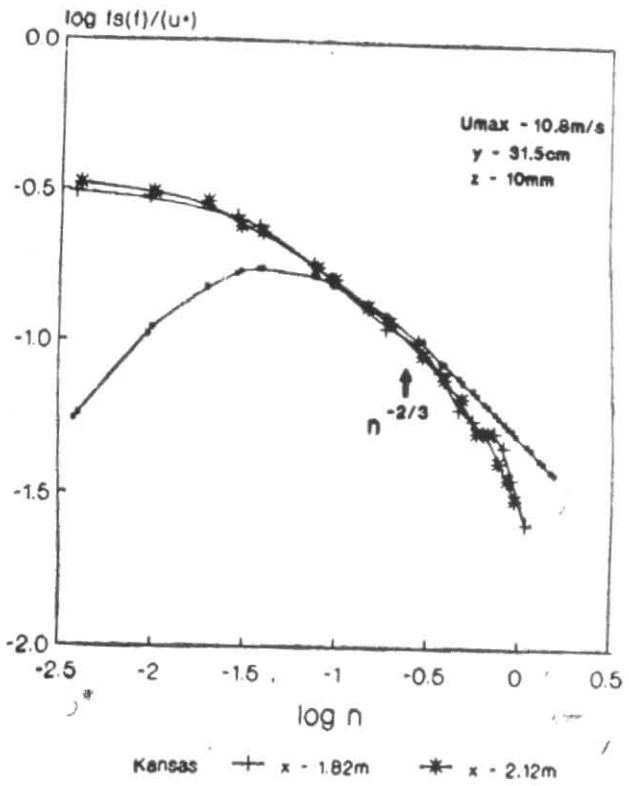

Fig. 7(a). Spectrum of longitudinal turbulence at 10 mm above tunnel floor

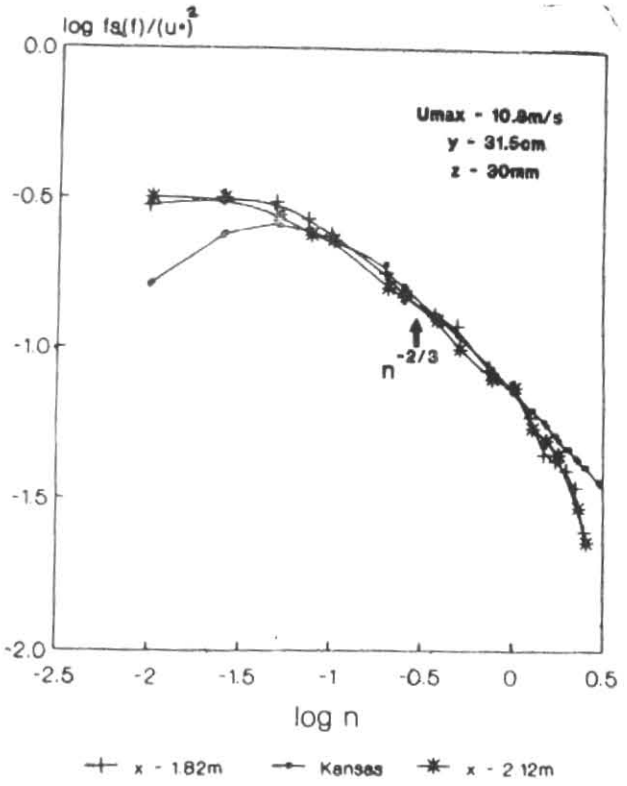

Fig. 7(b). Spectrum of longitudinal turbulence at 30 mm above tunnel floor

stress at 4 mm is measured as 2×10^{-3}. The stress in the logarithmic layer is nearly constant with a mean value of about 0.002 within a deviation of $\pm 10\%$. Above the logarithmic layer the stress decreases with height as in the atmospheric boundary layer.

3.3. *Streamwise turbulence spectrum*

Fig. 7(a) depicts logarithm of normalised streamwise (longitudinal) spectral density against logarithm of dimensionless frequency ($n = fZ/u$ where u is local mean streamwise velocity and f is the cyclic frequency in Hz.), at 10 mm above tunnel floor at mid-span for downstream locations 1.82 and 2.12 m from HFP. Figs. 7 (b & c) depict the corresponding spectral density at 30 and 100 mm above the tunnel floor. Longitudinal spectra obtained under neutral atmospheric conditions over uniform, flat and relatively featureless terrain in Kansas (Kaimal *et. al.* 1972) is plotted for comparison with simulated spectra. In engineering applications, most commonly used form of the spectrum is the Kansas spectrum, given by :

$$\frac{f S_u(f)}{u_*^2} = \frac{105\, n}{(1 + 33\, n)^{5/3}} \tag{3}$$

Comparison with simulated spectrum by reducing Eqn. (3) as

$$\frac{f S_u(f)}{u_*^2} = c\, \frac{105\, n}{(1 + 33\, n)^{5/3}} \tag{4}$$

where c which is a proportionality factor, yields good agreement for $c = 1/6$ in Fig. 7(a) and $c = 1/4$ in Figs. 7(b) & (c). The simulated spectra [Figs. 7(a–c)] depict the $-2/3$ law of Kolmogoroff in the inertial subrange of the spectrum. In Figs. 7 (a) & (b) due to Eqn. (4) the simulated spectra appear to show higher energy than the corresponding Kaimal spectra, at the low frequency end. The low frequency limit of the spectral analyser (2 Hz) restricts the measurement of spectral density values at frequencies much less than the peak (which lies in the 2–5 Hz frequency band). At the high frequency end, the spectral energy falls sharply due to filter characteristics of the spectrum analyser compared to the smoothed Kaimal spectra.

4. Assessment of simulation

The prime objective of modelling the characteristics of velocity profiles and turbulence in the wind tunnel is to use them efficiently to study the problems like wind flow over obstacles (like hills and mountains) and turbulent transport and diffusion of pollutant particles in the atmospheric boundary layer. In simulating wind profiles of the adiabatic atmospheric boundary layer, it is usually assumed that mechanical turbulence predominates thermal turbulence. Regarding similarity requirements (Cermak 1970) to be satisfied between the tunnel model and the prototype atmosphere, the Rossby number similarity is relaxed for the model flow. The Reynolds number similarity is satisfied by establishing that the wind tunnel boundary layer flow is fully rough.

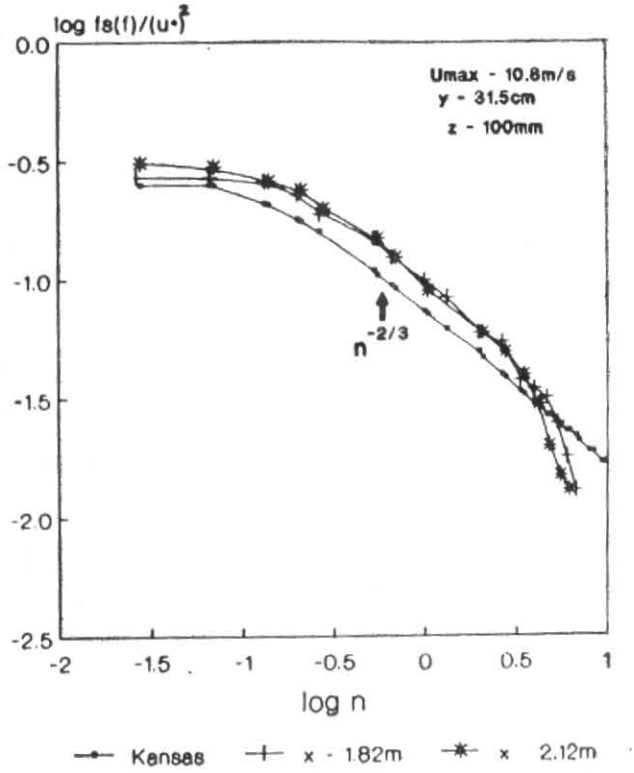

Fig. 7(c). Spectrum of longitudinal turbulence at 100 mm above tunnel floor

This is done using Nikuradse's (Sutton 1953) criterion :

$$\frac{u_* Z_o}{\nu} \geqslant 2.5 \qquad (5)$$

where, ν is the kinematic viscosity of air. Based on Reynolds stress measured close to the floor u_* is obtained from the relation :

$$(-\overline{u'w'} / U^2_{max}) = (u_*/U_{max})^2 \qquad (6)$$

and using this in equation (2), $u_* Z_0/\nu$ has been determined to be about 40 which shows that the tunnel flow is fully rough.

Matching the boundary layer height simulated in the tunnel (320 mm) with the atmospheric boundary layer height will be a crucial exercise. At high wind speeds (5-7 m/s at 10 m height) the gradient height has been taken as reference to represent the height of the adiabatic atmospheric boundary layer, in engineering literature. On the basis of theory and observations made in mid-latitude regions during the period 1880-1972, Counihan (1975) recommends a value of 600 m as the average height of both rural and urban boundary layer under adiabatic conditions. In tropics this height may vary and can be as high as 1-1.5 km, under neutral conditions. Hence matching boundary layer heights shall yield different and also large scale factors. It is also customary in application oriented problems to describe the wind profiles in terms of power laws. Hence fitting the simulated wind profiles to well known power laws (as in Fig. 2) give a general idea of terrain type to which these distributions of wind speeds have similarity.

The profiles exhibiting logarithmic linear variation with height upto 80 mm above tunnel floor ensures resemblance of wind profiles to adiabatic atmospheric profiles. Notwithstanding, it is essential that the structure of the model flow, *viz*, the cascading of turbulent energy and the size of eddies, have to be compared with atmospheric flow under similar situations so as to estimate a suitable scale factor. Counihan (1975) lists a range of values for longitudinal turbulence intensity at 30m above ground and the Reynolds stress near the ground over rural terrain :

$$0.10 \leqslant (\sqrt{\overline{u^2}}/U)_{30m} \leqslant 0.20$$

$$0.002 \leqslant (-\overline{u'\omega'}/U^2_{max}) \leqslant 0.0025$$

It is observed that the measured profiles of intensity of turbulence fall in this range in the vicinity of tunnel floor $Z/\delta=0.1$. Also the Reynolds stress close to the floor ($Z/\delta=0.1$) is about 0.002.

The roughness length Z_0 and the longitudinal integral length of the streamwise component of turbulence L^x_u which is a measure of dominant eddy size in turbulence, form the two key parameters that describe the mean velocity and the turbulence characteristics over the depth of simulation (Cook 1978). The roughness length Z_0 has an unique value in any given boundary layer but the integral length L^x_u is a function of height above ground and can be determined from correlation or spectral measurements. Table 1 gives the value of L^x_u obtained for the simulated spectra using the Von Karman model (Teunissen 1970)

$$L^x_u = 0.146/K \qquad (7)$$

where, K is the wave number corresponding to the peak value of non-dimensional spectrum.

Many workers expressed the variation of L^x_u with height by the relation

$$L^x_u \simeq Z^a \qquad (8)$$

For heights above 300 m the length scales are independent of terrain type (Teunissen 1970) in the atmosphere The relation ;

$$L^x_u = 20\sqrt{Z} \qquad (9)$$

is proposed by Teunissen (1970) on the basis of available results and it holds good in the 0-60 m hieght range. Table 1 shows the linear scaling for simulation corresponding to $Z=60$ m in Eqn. (9). The choice of maximum height range for which Eqn. (9) applies yields the maximum scale ratio so that a minimum geometric dimension could be estimated for the elements (for example, a stack) to be scaled in a desired type of flow.

Consequent upon the variation of L^x_u with height the scale ratio varies in Table 1. Overall, a linear scale of about 1:900 could be a judicious estimate between the simulated flow and the atmospheric surface layer flow. Based on this scaling we obtain a full scale height of 72 m corresponding to 80 mm height of logarithmic layer simulated and a roughness length of 0.09 m. These values along with turbulence intensity and the Reynolds stress measured in the tunnel agree

reasonably well with the corresponding values reported in the literature (Counihan 1975) for a typical rural terrain.

TABLE 1

Z (mm)	L^x_u (m)		Linear Scale L^x_u model : atmos
	x=1.82m	2.12 m	
10	0.153	0.150	1:1040
30	0.180	0.176	1:890
100	0.222	0.216	1:720

Further experiments on lateral and vertical turbulence spectra and the corresponding length scales will enlighten some more aspects on the structure of turbulence in the simulated flow. Studies of the present type have application in problems like wind effects on stability of tall structures, wind energy generation (design of propeller blades and location of them in turbulent field of flow) and modelling of the dispersion of air pollutants by eddy transport and diffusion in the laboratory—the studies of the kind have been progressing elsewhere.

5. Summary

The mean wind and turbulence characteristics produced in a short test-section wind tunnel show that :

(a) A system of barriers *viz.* cylindrical rods and a grid of Honeycomb Flat Plate designed for this study is a good combination of simple devices to model the flow structure of the adiabatic atmospheric boundary layer.

(b) The simulated wind profiles have similarity to neutral atmospheric boundary layer profiles. The height of the logarithmic layer, the surface stress, the profile of the longitudinal turbulence intensity and the roughness length agree well with the range of atmospheric values typical over rural terrain.

(c) The spectra of longitudinal turbulence closely follow the atmospheric spectra. The integral scale of longitudinal turbulence in the tunnel boundary layer increases with height as in the surface boundary layer of the atmosphere.

(d) On a scale of 1:900 the tunnel flow compares well with the prototype atmosphere and hence could be used to model the turbulent flow of the neutral surface boundary layer.

Acknowledgements

Authors are thankful to the Director, CWPRS, Khadakwasla for extending the wind tunnel facility, Officers and Staff of Cavitation Laboratory, CWPRS for cooperation during the experiment; the Director, Indian Institute of Tropical Meteorology, Pune, for the interest in the study.

References

Cermak, J.E., 1970, "Laboratory simulation of the atmospheric boundary layer," AIAA Paper No. 70-750.

Cook, N.J., 1978, "Wind tunnel simulation of the adiabatic atmospheric boundary layer by roughness barrier and mixing devices methods," *J. Ind. Aerodyn.*, **3**, 157-176.

Counihan, J., 1969, "An improved method of simulating an atmospheric boundary layer in a wind tunnel" *Atmos. Envir.*, **3**, 197-214.

Counihan, J., 1975, "Adiabatic atmospheric boundary layers : A review and analysis of data from the period 1880-1972," *Atmos. Envir.*, **9**, 871-905.

Harris, R.I., 1968, "Measurements of wind structure at heights up to 598 ft above ground level," Conf. on wind loads on buildings, Loughborough Univ.

Kaimal, J.C., Wyngaard, J.C., Izumi, Y. and Cote, O.R., 1972, "Spectral characteristics of surface layer turbulence," *Quart J. R. Met. Soc.*, **98**, 563-589.

Lawson, T.V., 1968, "Methods of producing velocity profiles in wind tunnel", *Atmos. Envir.*, **2**, 73-76.

Lloyd, A.R., 1967, "The generation of shear flow in a wind tunnel, *Quart. J. Roy. Met. Soc.*, **93**, 79-96.

Okamoto, S., 1986, "Turbulent shear flow behind rows of square plates placed on a plane boundary," *Atmos. Envir.*, **20**, 8, 1537-1546.

Okamoto, S., 1987, "Turbulent shear flow behind a single row of bluff obstacles placed on a plane boundary," *Atmos. Envir.*, **21**, 6, 1295-1303.

Sivaramakrishnan, S., 1980, "Mean wind velocity profiles in an artificially thickened boundary layer," *J. Indian Inst. Sci.*, **62** (A), 89-99.

Sutton, O.G., 1953, *Micrometeorology*," Mc.Graw Hill, New York, p. 82.

Taylor, G.I., 1960, "*The scientific papers of G.I. Taylor*," Cambridge University Press, 2, 288-315.

Teunissen, H.W., 1970, "Characteristics of mean wind and turbulence in the planetary boundary layer," UTIAS Review No. 32.